The Hard X-ray Imager (HXI) for the ASTRO-H mission

Goro Sato[a], Motohide Kokubun[b], Kazuhiro Nakazawa[c], Teruaki Enoto[d], Yasushi Fukazawa[e], Atsushi Harayama[b], Katsuhiro Hayashi[b], Jun Kataoka[a], Junichiro Katsuta[e], Madoka Kawaharada[b], Philippe Laurent[f], Francois Lebrun[f], Olivier Limousin[f], Kazuo Makishima[c], Tsunefumi Mizuno[e], Kunishiro Mori[b], Takeshi Nakamori[g], Hirofumi Noda[d], Hirokazu Odaka[b], Masanori Ohno[e], Masayuki Ohta[b], Shinya Saito[b], Rie Sato[b], Hiroyasu Tajima[h], Hiromitsu Takahashi[e], Tadayuki Takahashi[b], Shin'ichiro Takeda[b], Yukikatsu Terada[i], Hideki Uchiyama[j], Yasunobu Uchiyama[k], Shin Watanabe[b], Kazutaka Yamaoka[h], Yoichi Yatsu[l], Takayuki Yuasa[d], and the HXI team

[a]Research Institute for Science and Engineering, Waseda University, 3-4-1 Okubo, Shinjuku, Tokyo 169-8555, Japan;
[b]Institute of Space and Astronautical Science, Japan Aerospace Exploration Agency, 3-1-1 Yoshinodai, Chuou, Sagamihara, Kanagawa 252-5210, Japan;
[c]Department of Physics, University of Tokyo, 7-3-1 Hongo, Bunkyo, Tokyo 113-0033, Japan;
[d]RIKEN, Nishina Center for Accelerator-Based Science, 2-1 Hirosawa, Wako, Saitama 351-0198, Japan;
[e]Department of Physical Science, Hiroshima University, Higashi-Hiroshima, Hiroshima 739-8526, Japan;
[f]IRFU / Service d'Astrophysique, CEA Saclay, 91191 Gif-sur-Yvette Cedex, France;
[g]Department of Physics, Faculty of Science, Yamagata University, Kojirakawa, Yamagata 990-8560, Japan;
[h]Solar Terrestrial Environment Laboratory, Nagoya University, Chikusa, Nagoya, Aichi 464-8601, Japan;
[i]Department of Physics, Saitama University, Saitama, Saitama 338-8570, Japan;
[j]Science Education, Faculty of Education, Shizuoka University, Suruga, Shizuoka, 422-8529, Japan;
[k]Department of Physics, Rikkyo University, Toshima, Tokyo, 171-8501, Japan;
[l]Department of Physics, Tokyo Institute of Technology, Meguro, Tokyo 152-8551, Japan

ABSTRACT

The 6th Japanese X-ray satellite, ASTRO-H, is scheduled for launch in 2015. The hard X-ray focusing imaging system will observe astronomical objects with the sensitivity for detecting point sources with a brightness of 1/100,000 times fainter than the Crab nebula at > 10 keV. The Hard X-ray Imager (HXI) is a focal plane detector 12 m below the hard X-ray telescope (HXT) covering the energy range from 5 to 80 keV. The HXI is composed of a stacked Si/CdTe semiconductor detector module and surrounding BGO scintillators. The latter work as active shields for efficient reduction of background events caused by cosmic-ray particles, cosmic X-ray background, and in-orbit radiation activation. In this paper, we describe the detector system, and present current status of flight model development, and performance of HXI using an engineering model of HXI.

Keywords: X-ray Astronomy, Hard X-ray Imager, ASTRO-H mission

Send correspondence to G.S., E-mail: gsato@aoni.waseda.jp

Space Telescopes and Instrumentation 2014: Ultraviolet to Gamma Ray, edited by Tadayuki Takahashi, Jan-Willem A. den Herder, Mark Bautz, Proc. of SPIE Vol. 9144, 914427 · © 2014 SPIE
CCC code: 0277-786X/14/$18 · doi: 10.1117/12.2055629

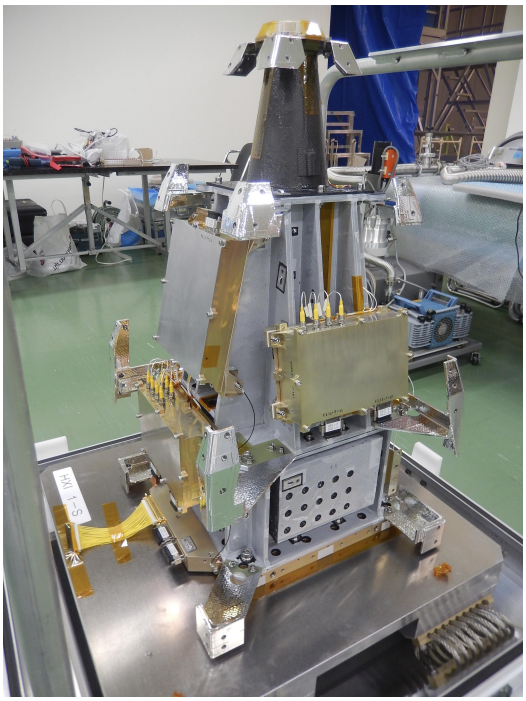

Figure 1. Sensor part of Hard X-ray Imager (HXI-S) before installation.

1. INTRODUCTION

The Hard X-ray Imager (HXI), shown in Figure 1, is a highly sensitive hard X-ray imaging instrument, utilizing active shield technique as part of the hard X-ray imaging system on board the ASTRO-H mission.[1–3] The HXI is designed to perform hard X-ray imaging spectroscopy in conjunction with the hard X-ray super mirror (Hard X-ray Telescope: HXT))[4–6] in the energy range from 5 to 80 keV within a field-of-view of 9 arc minutes. The overall effective area is expected to be > 300 cm^2 in total at 30 keV. The HXI instrument is being built, and integrated with the ASTRO-H spacecraft at Japan Aerospace Exploration Agency (JAXA). The launch of ASTRO-H is scheduled for 2015.

The hard X-ray imaging system consists of two sets of the HXT, fixed and extendable optical benches, and two identical detectors, located at focal points of the two HXTs. The HXT is designed to have a long focal length of 12 m to maximize its effective area at an energy of 30 keV. Since it is difficult to fit such a long fixed optical bench (FOB) in the launch vehicle, an extendable optical bench (EOB), whose length is increased by 6 m in orbit, is employed. While the telescopes are mounted on the top plate of the FOB, the two detectors are on a plate, called HXI-plate, attached to the far end of the EOB. The power supply and signal cables which connect the detector to the spacecraft bus also have to be extended, and are laid out with special consideration to the thermal and mechanical interface between the detector and spacecraft bus system. The basic parameters describing the HXT-HXI system are listed in Table 1. See previous papers[7–10] for the design concept and requirements for the HXI.

One HXI consists of four boxes, HXI-S, HXI-AE, HXI-DPU, and HXI-DE. The sensor part, HXI-S, is mounted on a cold plate with temperature control heaters and heat-pipes connected to the radiator. The HXI-S has a weight of 43 kg and is the heaviest due to the thick BGO crystals. A housing structure made of carbon fiber reinforced plastic (CFRP) holds the entire volume in which all the BGO and APD units are mechanically supported. High-voltage units and charge sensitive preamplifiers for the APDs are assembled to the CFRP housing. The HXI-AE consists of two circuit boards, the Camera Power Management Unit (CPMU) and the APD Processing and Management Unit (APMU).

Table 1. Basic parameters describing the HXT-HXI system onboard ASTRO-H

Energy range	5–80 keV
Field of view	$9.17' \times 9.17'$
Half power diameter of mirror	$\sim 2'$
Effective area	> 300 cm^2 @30 keV
Imaging area	32 mm $\times$ 32 mm
Spatial resolution	250 μm $= 0.07'$
Energy resolution	< 2 keV (FWHM)

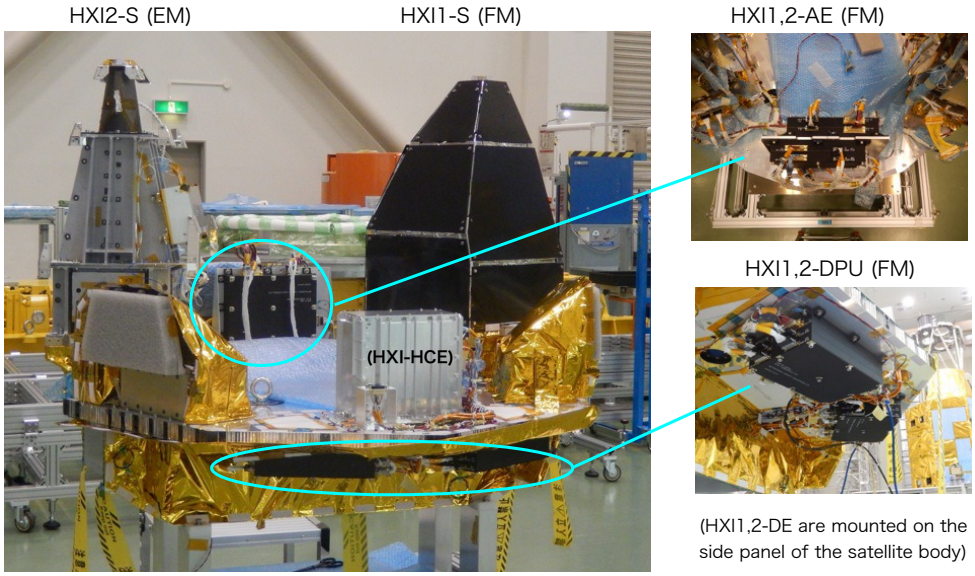

Figure 2. Pictures from the electronics integration test held at JAXA Tsukuba Space Center.

The CPMU controls the power supply to the front-end electronics and high-voltage modules of the imager assembly, and also monitors the temperatures and output voltages. Scintillation photons from the BGO crystals are read by individually attached APDs, and amplified in the APD pre-amplifiers. The signals from the pre-amplifiers are processed and digitized in the APMU. The digital data from the imager trays, the CPMU, and the APMU are fed into the HXI-DPU, which contains two identical FPGA boards and one power supply module. The data are processed and recorded in the local memory of the HXI-DPU, until the data are transferred by software running on a CPU contained in the HXI-DE. After being buffered and formatted into the standard data structure, the data are finally copied to the data recorder of the spacecraft.

2. CURRENT STATUS OF HXI

Manufacture of the first flight model of HXI-S (HXI1-S) was completed in February 2014 (Figure 1). Components of HXI2-S have been manufactured and will be assembled by the end of July 2014. The flight model of electronics boxes (HXI-AE, HXI-DPU, and HXI-DE) have also been manufactured and delivered to the satellite for mechanical and electrical integration tests at JAXA Tsukuba Space Center. Figure 2 shows pictures from the integration test. The flight model of HXI1-S covered by sun-shade panels was mounted on the HXI-plate which will be attached to the end of EOB. For HXI2-S, an engineering model instead of the flight model was mounted at this moment. During a detailed function test, two sets of HXI were operated continuously for 24 hours together with other mission instruments (Soft X-ray Spectrometer: SXS, Soft X-ray Imager: SXI; Soft

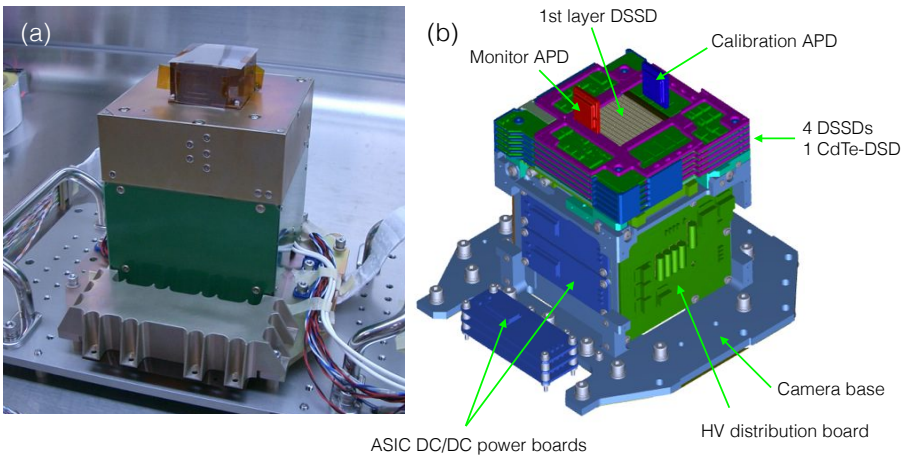

Figure 3. (a) Picture of the engineering model of the HXI camera (b) A 3D model of the HXI camera showing inner components.

Gamma-ray Detector: SGD) and bus equipments of the satellite. No significant issues such as interferences were found for HXI.

After the integration test, the two sets of HXI were demounted from the satellite for refurbishment and for further environmental testing. The sensor part and electronics boxes will be refurbished for final coating of electronics boards, and for fixing cables etc. Mechanical vibration, thermal cycle, and vacuum testing are planned for acceptance certification. The vibration testing includes broadband random environment precipitating impending failures due to workmanship defects, and sine sweeps to identify resonances. Acoustic testing is also planned for HXI-S, simulating acoustic or aerodynamic pressures inside a rocket at launch. After calibrating detectors, all the components will be mounted on the satellite again, and further environmental/electronic testing will be conducted in preparation for the launch in 2015.

3. HXI SENSOR (HXI-S)

3.1 HXI Camera

The HXI camera is an imager assembly composed of four double-sided silicon strip detectors (DSSDs), and a cadmium telluride double-sided strip detector (CdTe-DSD). A picture of the engineering model of the HXI camera, and its 3D model are shown in Figure 3. The Si/CdTe detectors are designed to be readout by identical ASICs and mounted on identical sensor trays, which was a key modular feature enabling fast and efficient development of the HXI camera. The sensor trays are vertically stacked on an aluminum camera base so that the CdTe-DSD is located in the bottom. Photons of energy less than $\sim$30 keV will be primarily absorbed in the DSSDs, whereas higher energy photons will be detected in the CdTe detector below.

The DSSD used in HXI is a well-established device developed with Hamamatsu Photonics, Japan, based on our past extensive studies (e.g.[11–13]). The geometrical size of the device is roughly 32×32 mm which consists of 128 readout strips for each p- and n-side orthogonally oriented. The device was produced from an n-type wafer, and a floating p-implantation was made between strips on n-side to isolate adjacent strips. The strip pitch is 250 μm with a strip gap of 50 μm. The CdTe-DSD is newly developed with ACRORAD, Japan, based on our technology of CdTe diode detectors.[14–17] The detector size is about 32×32 mm with the thickness of 0.75 mm. The cathode strips are made of platinum and the anode strips are made of aluminum, forming a diode type contact. The strip pitch is 250 μm and a strip gap is 20 μm. Energy response of CdTe-DSD is studied in Hagino et al.[18] See also our previous papers[19,20] for polarization effect in Schottky CdTe diodes. The low-noise front-end ASICs were developed in collaboration with GM-IDEAS.[17,21]

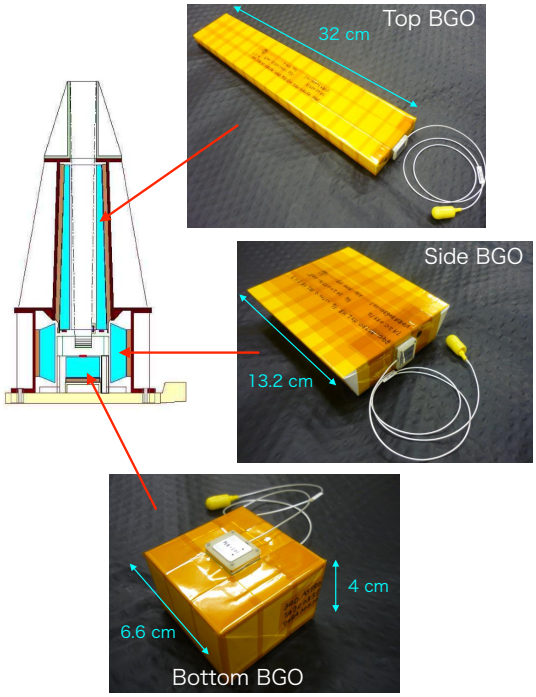

Figure 4. Pictures of BGO and APD units prepared for HXI-S (flight model).

Because the sensors are DC-coupled to the ASICs on both p, and n-sides, a floating readout method is adopted. The sensor tray is divided in two regions where the n-side is floated up to the high voltage level. For power supply of ASICs, isolation-type DC/DC converters are required for n-side while linear regulators are used for p-side. In order to minimize external noise, the power boards are placed close to the sensors. A high voltage distribution board is also attached to the camera base.

On the top of the HXI camera, two avalanche photodiode (APD) assemblies are attached. One is for cosmic-ray monitoring, and the other is coupled with a plastic scintillator doped with ^{241}Am, working as a tagged source for onboard energy calibration of Si/CdTe detectors. The calibration sources were fabricated in CEA lab. To reduce the risk of increasing background in case of the APD malfunction, the activity of the source is kept quite low: 3.365 Bq for HXI-1 and 4.088 Bq for HXI-2. The low energy photons, at around 15–25 keV are used for the DSSDs, while those at 60 keV are used primarily for the CdTe-DSD.

3.2 BGO active shield and Avalanche Photo Diode (APD)

Active rejection of cosmic-ray particles with a BGO scintillator plays an important role in obtaining an unprecedented sensitivity with the in-orbit observations. Since the shield also works as the Compton suppression, it is also important to achieve as low energy threshold as possible.

The active shield is made of 9 units of BGO crystals to cover the imager as a whole. Their total weight is 21.6 kg, and each unit has a weight of 1.2–3 kg. Figure 4 shows pictures of the BGO and APD units in three different shapes. To hold fragile crystals against the launch vibration, they are glued on to a plate made of hybrid carbon fiber and glass fiber reinforced plastic (CFGF). The CFGF is specially designed to have a coefficient of thermal expansion of 6×10^{-6} K^{-1}, similar to that of the BGO crystal (7×10^{-6} K^{-1}). The glue also has some elasticity. The BGO of the gluing side is painted with a BaSO4 reflector, referring to those utilized in the HXD of Suzaku.[22] Other 5 sides of the crystal is covered with a ESR reflector of 3M, and a 250 μm thick white GoreTex sheet, packed with a poly-imid tape.

As scintillation light sensors, reverse-type Avalanche Photo-Diodes (APDs) developed in collaboration with Hamamatsu photonics are employed.[23–25] When compared with the canonical photo-multiplier tubes, a sig-

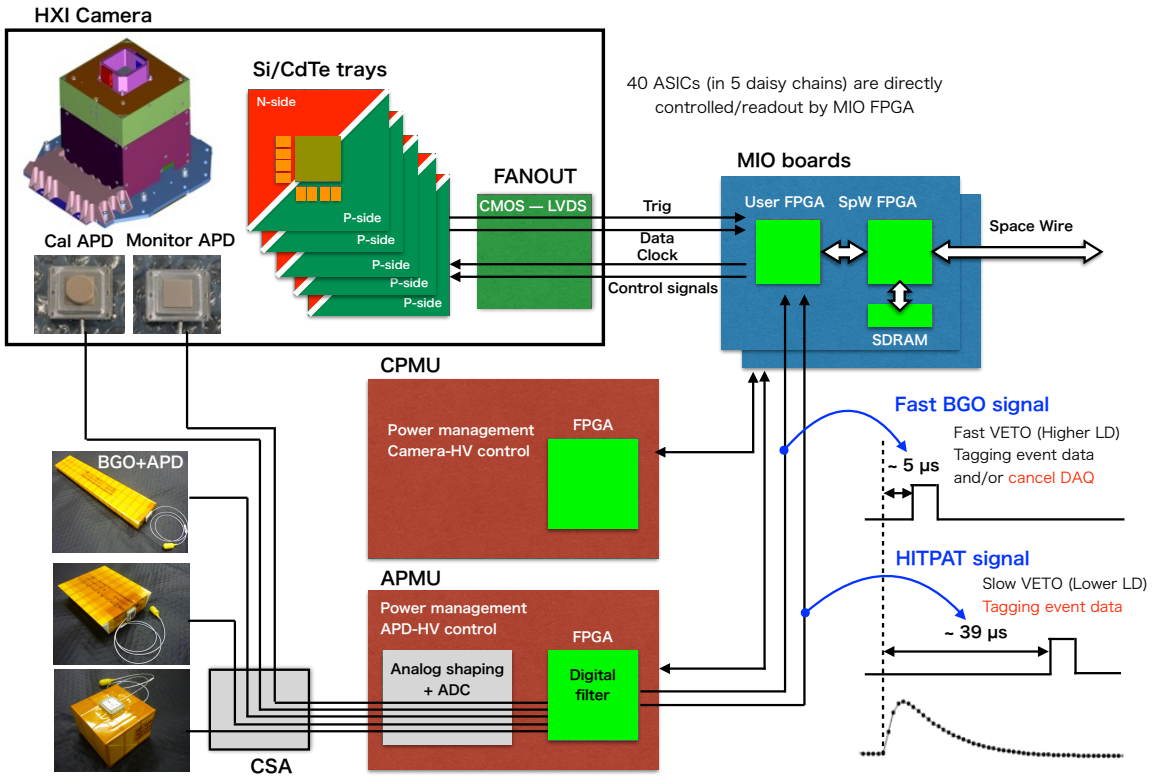

Figure 5. Readout system of the HXI instrument.

nificantly lower high-voltage required helps to design the flight electronics, in terms of in-orbit discharges. In addition, the compact size of the APD enables us to separate the BGOs into 9 parts, with limited leakage clearance. Without the APDs, it will be needed to optically glue the BGOs to shield the 10 cm wide imager assembly, and hence the weight of a BGO unit will become as heavy as 10 kg or more. In this case, the mechanical design would be much difficult. The APD is assembled in an aluminum shield and then glued to the BGO. Combined with the specially designed pre-amplifier and dedicated analog chain in the APMU board, the lower threshold of the BGO active shield is estimated to reach 80–100 keV.

4. READOUT SYSTEM

The readout system of the HXI instrument is represented in Figure 5. Each sensor tray has 8 ASICs to readout both sides the Si/CdTe detectors. The ASICs are daisy-chained in each board, and are controlled and readout directly by an FPGA on a digital processing board called as MIO (Mission I/O) board. Control and clock signals are sent from the FPGA to the ASICs, while data from the imaging sensors are immediately digitized in analog-to-digital converters embedded in the ASICs, and delivered to the same FPGA. The digital signals are single-ended inside the HXI camera, while converted to differential in the fanout board beneath the stacked sensor trays to minimize the electromagnetic interference during communicating between the HXI-Camera and the MIO board.

Signals from the active shields and calibration/monitor APDs are amplified in charge sensitive amplifier (CSA) boxes attached to HXI-S, and then fed into the APMU board. APMU has analog processing circuits followed by 12-bits flash ADCs for digital sampling at the frequency of 15/16 MPS. An FPGA on the APMU board has a function of digital filtering and output two types of VETO signals. One is Fast BGO signal generated within 5 μs after the event, which is used for tagging event data, and/or canceling data acquisition by the MIO FPGA, which reduces dead time of observations. The other is HITPAT signal generated in typically 39 μs using

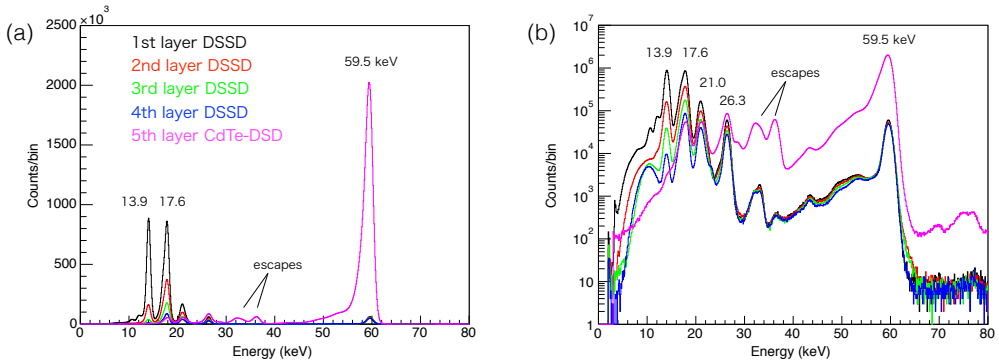

Figure 6. ^{241}Am spectra obtained with the engineering model of the HXI camera shown in (a) linear and (b) logarithmic scales. Data from all the 128 channels are added on the p-side for DSSDs, and on the Al-side for CdTe-DSD.

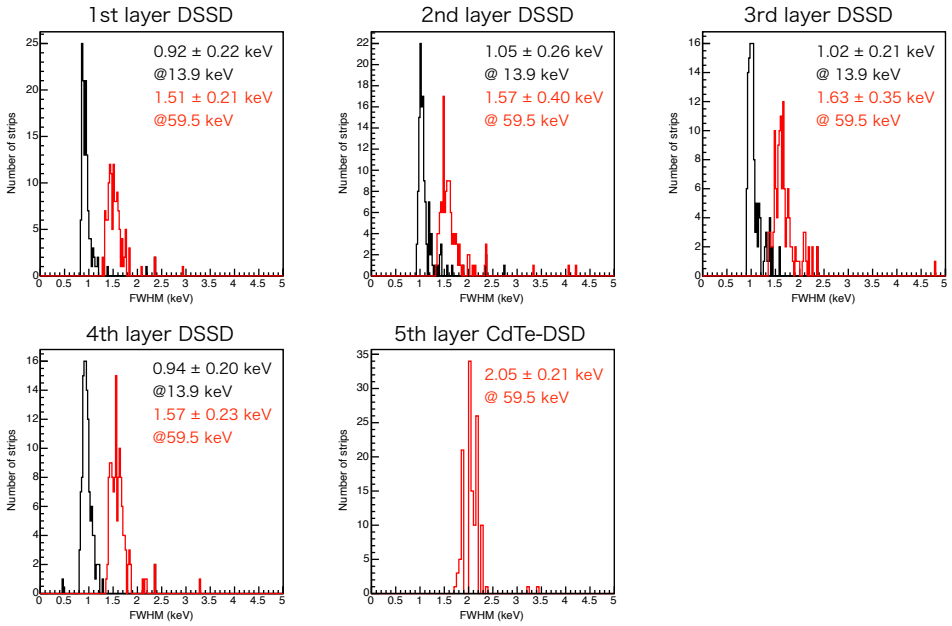

Figure 7. Distributions of strip-by-strip energy resolutions for the Si/CdTe detectors.

better digital filtering with larger number of taps, which is used for tagging event data. The information tagged to event data are useful for offline event selection. See Ohno et al.[26] for more details of signal processing of the active shields.

5. PERFORMANCE OF THE ENGINEERING MODEL

Since refurbishment and further environmental testing are ongoing for the flight model of HXI, dedicated measurements with the detectors at cool environment will be performed at a later point. In this section we present experimental results obtained with an engineering model of HXI which contains a full set of the sensors: stacked Si/CdTe detectors, 9 BGO units, and calibration/monitor APDs.

The engineering model was placed inside a thermostatic chamber and operated at −20°C. The applied bias voltage was 300 V and 250 V for DSSDs and CdTe-DSD, respectively. Figure 6 shows spectral performance of the engineering model of the HXI camera obtained with an ^{241}Am radioactive source. The energy resolutions of DSSDs are measured as 0.9, 1.1, 1.0, and 1.0 keV (FWHM) at 13.9 keV lines from upper to lower layers,

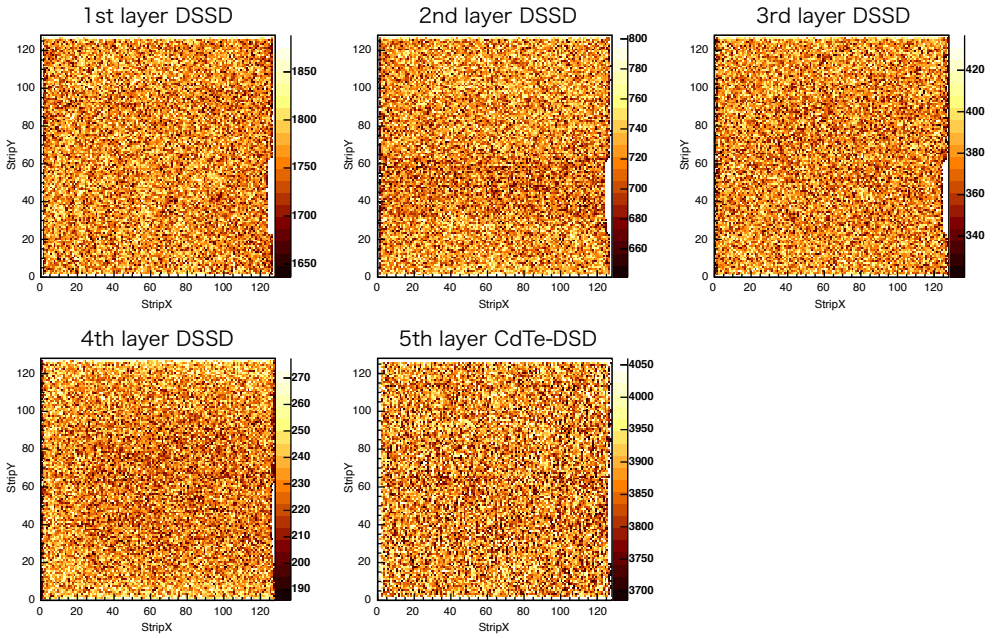

Figure 8. Detector images in the energy range from 5 to 85 keV for flood illumination of gamma-rays from an ^{241}Am source.

respectively. The resolution of CdTe-DSD is 2.0 keV (FWHM) at 59.5 keV. In the spectrum of CdTe-DSD, escape peaks can be seen as a result of escaping fluorescent X-rays: 23 keV from cadmium and 26 keV from tellurium. Since the readout system simultaneously latches signals from all the layers, events with interactions in multiple layers can be recorded. Some of fluorescent X-rays from CdTe are detected in upper Si layers. These events will be properly handled in the data processing pipeline of HXI. While this detector originated line is excluded from a DSSD spectrum, events with combined energies are added in a CdTe spectrum. For the measurement with the ^{241}Am source, 84% of 2-layer hit events were such events. Other 2-layer events mainly due to Compton scattering inside the HXI camera were excluded.

The energy resolutions were measured strip by strip, and the distributions are shown in Figure 7. The requirement of energy resolution for Si/CdTe is 2.0 keV (FWHM). For the 1st layer DSSD, the median is 0.92 keV and 1.51 keV (FWHM) for 13.9 keV and 59.5 keV lines, showing that the DSSD have much better energy resolution than the requirement in the whole energy band of HXI. Outliers are only the edge strips. For the 5th layer CdTe-DSD, the energy distribution is distributed around the requirement with the median of 2.05 keV. Outliers are only the edge strips also for the CdTe-DSD.

Detector images in the energy range from 5 to 85 keV are shown in Figure 8. The detected counts are filled in each pixel cell at cross points of p- and n-side strip signals. The range of color maps is adjusted to $\pm 3\sigma$ of the mean counts. The images are mostly flat except for the while pixels on the right edge of each layer, which have much lower counts. This is due to a shadow of the calibration APD, which is not a problem but just as designed. To keep tight shielding of the main detectors by the BGO units, we have decided to place the calibration APD on the edge of the imaging area in the limited spaces. The distribution of pixel counts were evaluated with a gaussian function for each layer. Standard deviation other than statistics is calculated as 0.4, 1.0, 0.6, 1.8, and 1.2% from upper to lower layers, respectively.

Figure 9 shows background spectrum measured for 12 hours on ground. Firstly, event selection was performed by the information of number of hit layers. For this measurement, 77% of all the hit events are recorded as single layer hit events. Others are multi-layer hit events, including 5.7% of 5 layer hit events, that are likely caused by cosmic-ray penetrating all the detectors. Here, we selected single layer hit events and also two layer hit events due to fluorescent X-rays from CdTe as described above. In Figure 9, extracted spectra are shown in black, where

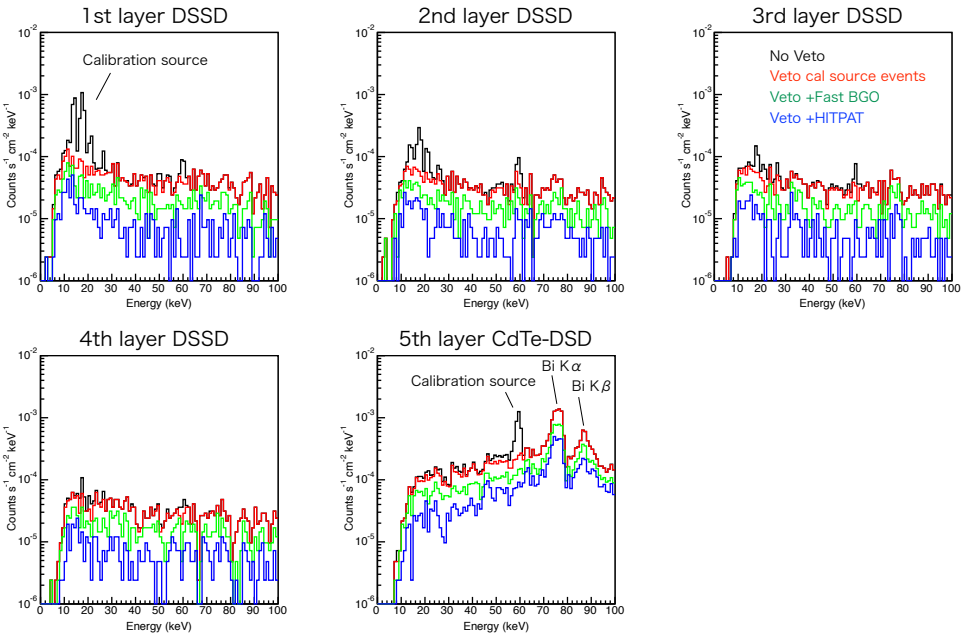

Figure 9. Background spectra on ground obtained with the fully-equipped engineering model of HXI.

emission lines from the calibration source are observed. Secondly, event selection was performed using tagged information based on the veto signals from the active shields. By vetoing events tagged by the calibration APD, the emission lines from the calibration source are properly excluded as shown in red spectra. We further excluded events tagged by Fast BGO and HITPAT signals, and finally obtained spectra shown in blue. The background level reaches approximately 10^{-5} and 10^{-4} counts cm^{-2} s^{-1} keV^{-1} for DSSDs and CdTe-DSD, respectively, verifying that the signal processing of anti-coincidence technique is working properly.

6. SUMMARY

We have finalized the design of the HXI instrument including all the electronics boxes. The flight models are being built and integrated with the satellite. The imager assembly is called as HXI camera containing 4 DSSDs and 1 CdTe-DSD in vertically stacked configuration. The camera is surrounded by 9 BGO scintillators, which works as active shield for background rejection using anti-coincidence technique. The entire system is working properly for the flight models. The fully equipped engineering model of HXI has been evaluated in the laboratory and the spectral performance, imaging performance, and low background property have been confirmed.

REFERENCES

[1] Takahashi, T., Mitsuda, K., and Kelley, R. L., *et al.*, "The ASTRO-H X-ray Observatory," *in [Space Telescopes and Instrumentation 2012: Ultraviolet to Gamma Ray], Proc. SPIE* **8443** (2012).

[2] Takahashi, T., Mitsuda, K., and Kelley, R. L., *et al.*, "The ASTRO-H mission," *in [Space Telescopes and Instrumentation 2010: Ultraviolet to Gamma Ray], Proc. SPIE* **7732** (2010).

[3] Takahashi, T., *et al.*, "The NeXT mission," *in [Space Telescopes and Instrumentation 2008: Ultraviolet to Gamma Ray], Proc. SPIE* **7011** (2008).

[4] Kunieda, H., *et al.*, "Hard X-ray Telescope to be onboard ASTRO-H," *in [Space Telescopes and Instrumentation 2010: Ultraviolet to Gamma Ray], Proc. SPIE* **7732** (2010).

[5] Awaki, H., *et al.*, "Current status of ASTRO-H hard x-ray telescopes (HXTs)," *in [Space Telescopes and Instrumentation 2012: Ultraviolet to Gamma Ray], Proc. SPIE* **8443** (2012).

[6] Ogasaka, Y., *et al.*, "The NeXT X-ray telescope system: status update," *in [Space Telescopes and Instrumentation 2008: Ultraviolet to Gamma Ray], Proc. SPIE* **7011** (2008).

[7] Takahashi, T., Awaki, A., Dotani, T., Fukazawa, Y., Hayashida, K., Kamae, T., J.Kataoka, Kawai, N., Kitamoto, S., Kohmura, T., Kokubun, M., Koyama, K., Makishima, K., Matsumoto, H., Miyata, E., Murakami, T., Nakazawa, K., Nomachi, M., Ozaki, M., Tajima, H., Tashiro, M., Tamagawa, T., Terada, Y., Tsunemi, H., T.Tsuru, K.Yamaoka, Yonetoku, D., , and Yoshida, A., "Wide band X-ray Imager (WXI) and Soft Gamma-ray Detector (SGD) for the NeXT Mission," *in [UV and Gamma-Ray Space Telescope Systems], Proc. SPIE* **5488** (2004).

[8] Kokubun, M., *et al.*, "The Hard X-ray Imager (HXI) for the NeXT mission," *in [Space Telescopes and Instrumentation 2008: Ultraviolet to Gamma Ray], Proc. SPIE* **7011** (2008).

[9] Nakazawa, K., *et al.*, "The Hard X-ray Imager onboard IXO," *in [Space Telescopes and Instrumentation 2010: Ultraviolet to Gamma Ray], Proc. SPIE* **7732** (2010).

[10] Kokubun, M., *et al.*, "The Hard X-ray Imager (HXI) for the ASTRO-H mission," *in [Space Telescopes and Instrumentation 2012: Ultraviolet to Gamma Ray], Proc. SPIE* **8443** (2012).

[11] Nakazawa, K., Takeda, S., Tanaka, T., Takahashi, T., Watanabe, S., Fukazawa, Y., Sawamoto, N., Tajima, H., Itoh, T., and Kokubun, M., "A high-energy resolution 4 cm-wide double-sided silicon strip detector," *Nuclear Instruments and Methods in Physics Research A* **573**, 44–47 (2007).

[12] Tajima, H., Kamae, T., Uno, S., Nakamoto, T., Fukazawa, Y., Mitani, T., Takahashi, T., Nakazawa, K., Okada, Y., and Nomachi, M., "Low-noise double-sided silicon strip detector for multiple-compton gamma-ray telescope," *in [X-Ray and Gamma-Ray Telescopes and Instruments for Astronomy], Proc. SPIE* **4851** (2003).

[13] Takeda, S., Watanabe, S., Tanaka, T., Nakazawa, K., Takahashi, T., Fukazawa, Y., Yasuda, H., Tajima, H., Kuroda, Y., Onishi, M., and Genbae, K., "Development of double-sided silicon strip detectors (DSSD) for a Compton telescope," *Nuclear Inst. and Methods in Physics Research, A* **579**, 859–865 (2007).

[14] Takahashi, T., *et al.*, "Recent Progress in CdTe and CdZnTe detectors," *IEEE Trans. Nucl. Sci.* **48**, 950–959 (2001).

[15] Ishikawa, S., Aono, H., Watanabe, S., Takeda, S., Nakazawa, K., and Takahashi, T., "Performance measurements of Al/CdTe/Pt pixel diode detectors," *in [Hard X-Ray and Gamma-Ray Detector Physics IX], Proc. SPIE* **6706** (2007).

[16] Watanabe, S., Ishikawa, S., and Takeda, S., *et al.*, "New CdTe Pixel Gamma-Ray Detector with Pixelated Al Schottky Anodes," *J.J.Appl.Phys.* **46**, 6043–6045 (2007).

[17] Watanabe, S., *et al.*, "High Energy Resolution Hard X-ray and Gamma-Ray Imagers Using CdTe Diode Devices," *IEEE Trans. Nucl. Sci.* **56**, 777–782 (2009).

[18] Hagino, K., *et al.*, "Imaging and spectral performance of CdTe double-sided strip detectors for the Hard X-ray Imager onboard ASTRO-H," *in [Space Telescopes and Instrumentation 2012: Ultraviolet to Gamma Ray], Proc. SPIE* **8443** (2012).

[19] Sato, G., Fukuyama, T., Watanabe, S., Ikeda, H., Ohta, M., Ishikawa, S., Takahashi, T., Shiraki, H., and Ohno, R., "Study of Polarization Phenomena in Schottky CdTe Diodes using Infrared Light Illumination," *Nuclear Inst. and Methods in Physics Research, A* **652**, 149–152 (2011).

[20] Takahashi, T., Watanabe, S., Ishikawa, S., Sato, G., and Takeda, S., "High-Resolution CdTe Detectors and Their Application to Gamma-Ray Imaging," in [*Biological and Medical Sensor Technologies*], Iniewski, K., ed., 339–366, CRC Press (2012).

[21] Tajima, H., Nakamoto, T., and Tanaka, T., *et al.*, "Performance of a Low Noise Front-end ASIC for Si/CdTe Detectors in Compton Gamma-ray Telescope," *IEEE Trans. Nucl. Sci.* **51**, 842–847 (2004).

[22] Nakazawa, K., *et al.*, "Fabrication of the ASTRO-E hard-x-ray detector ," *in [UV to Gamma-Ray Space Telescope Systems], Proc. SPIE* **3765** (1999).

[23] Kataoka, J., *et al.*, "Development of large-area, reverse-type APD arrays for high-resolution medical imaging," *Nuclear Inst. and Methods in Physics Research, A* **604**, 323–326 (2009).

[24] Kataoka, J., Saito, T., and Kuramoto, Y., *et al.*, "Recent progress of avalanche photodiodes in high-resolution X-rays and γ-rays detection," *Nuclear Inst. and Methods in Physics Research, A* **541**, 398–404 (2005).

[25] Kataoka, J., Saito, T., and Kuramoto, Y., *et al.*, "Development of 2 cm-square Hamamatsu avalanche photodiodes for high-resolution X-rays and γ-rays detection," *Nuclear Inst. and Methods in Physics Research, A* **556**, 535–542 (2006).

[26] Ohno, M., *et al.*, "Development and verification of signal processing system of BGO active shield onboard ASTRO-H," *in [Space Telescopes and Instrumentation 2014: Ultraviolet to Gamma Ray], Proc. SPIE* – (2014).